

## Swelling of Copolymer Micelles by Added Homopolymer

M. D. Whitmore\*

*Department of Physics, Memorial University of Newfoundland, St. John's, Newfoundland, Canada A1B 3X7*

T. W. Smith

*Xerox Corporation, Webster Research Center, Webster, New York 14580**Received November 8, 1993; Revised Manuscript Received May 10, 1994\**

**ABSTRACT:** We present a simple theory and a supporting experimental study of the extent to which block copolymer micelles in a homopolymer matrix can be swollen by relatively low molecular weight homopolymer which is compatible with the copolymer block that forms the micelle cores. The theory is an extension of simple models of copolymer micelles<sup>1-3</sup> and predicts the solubilization limit of the added homopolymer, its effects on the micelle size and number density, and the dependences of these quantities on the molecular weights and relative volume fractions of the constituents. The experiments were carried out on systems of PS-*b*-PEO block copolymers in PS hosts to which homopolymer PEO was added. The experimental results can be understood within the context of the theoretical picture.

## 1. Introduction

In recent years, there has been considerable experimental and theoretical interest in polymer blends in which at least one of the components is a block copolymer. Broadly speaking, one can think of two regimes which are delineated by the overall volume fraction of the copolymer,  $\phi_c$ . If the copolymer constitutes a relatively large fraction of the system, then an ordered microphase can form, and the usual questions of interest focus on the microphase separation transition (MST), the morphology and domain sizes of ordered microphases, and the overall phase behavior of the multicomponent system including the interplay between microphase and macrophase separation. The other regime is one in which the block copolymer represents a relatively small fraction of the entire system, typically on the order of 10% or less. One example is binary copolymer/homopolymer blends of the form A-*b*-B/A. The copolymer can form disordered micelles dispersed in the homopolymer matrix, with the incompatible B block forming the micelle cores which are surrounded by coronas consisting of the A block extending into the matrix of A homopolymer. In ternary copolymer/homopolymer/homopolymer blends in this regime, the usual focus has been on the use of the copolymer as surfactant at homopolymer/homopolymer interfaces.

Block copolymer micelles provide a mechanism for dispersing a minority component throughout a host matrix in domains with sizes that are generally smaller, and more monodisperse and controllable, than those which are obtained by mixing homopolymers. In this paper we study a combined process, namely the dispersion of material using both copolymer and homopolymer in the host. In particular, we consider binary blends with low concentrations of A-*b*-B copolymer which forms micelles in the A host homopolymer, to which low concentrations of B homopolymer are added.

Measurements of the physical characteristics of these systems, e.g., the critical micelle concentration (cmc), the micelle aggregation number and size, and the solubilization limit of the homopolymer, are difficult. They require precise low-angle X-ray scattering studies or time-consuming microscopy analyses of systems in their equilibrium state. Our goals here are to develop a simple model

which provides a straightforward computation of these properties with reasonable accuracy and to identify the primary physical factors controlling the behavior of the system. We also provide some experimental evidence which supports the predictions of the theory.

In regards to the disposition of the added B homopolymer, we examine the extent to which it is solubilized within the micelle cores rather than being expelled into a separate phase. This is discussed in terms of the solubilization limit of the homopolymer within the micelle cores. For concentrations below this limit, the theory predicts the effects of the solubilized homopolymer on the micellar core radii, the number of micelles per unit volume, the relative volume fraction within each core attributable to the copolymer and the homopolymer, respectively, and the number of copolymer and homopolymer molecules per micelle.

Similar theoretical pictures of copolymer micelles in binary copolymer/solvent and copolymer/homopolymer blends have been presented by Hong, Noolandi, and Whitmore<sup>1,2</sup> and Leibler, Orland, and Wheeler.<sup>3</sup> The theory presented here is an extension of these models, explicitly that of ref 2. These models are based on pictures of the micelles in which each region is considered uniform and for which simplified expressions for the free energy are developed and minimized. This kind of approach does not provide the level of detail available from more sophisticated theories of polymer systems, for example refs 4-11 and other references contained therein. On the other hand, such models can give direct insight into the governing characteristics, and they have in the past provided quite reasonable levels of agreement with experiment for quantities such as the micelle sizes and their dependences on the degrees of polymerization of each of the copolymer blocks and the homopolymer, all with little computational effort.<sup>2,12-14</sup>

The experimental system studied in this paper is comprised of poly(styrene-*block*-ethylene oxide) (PS-*b*-PEO) in polystyrene and swollen by poly(ethylene oxide). As will be discussed below, because of the marked immiscibility of polystyrene and the copolymers used in the swelling experiments, the cmc is much smaller than the overall copolymer concentrations used, and essentially all the copolymer is in micelles. This is a kind of "strong segregation regime", not uncommon in micelle systems. The formalism we develop here is for this limit but could

\* Abstract published in *Advance ACS Abstracts*, June 15, 1994.

**Table 1. PEO Micelles: Domain Size and Composite Properties<sup>a</sup>**

sample no. and comp (PS/PS- <i>b</i> -PEO/PEO) <sub>w</sub>	rel PEO vol frac		PEO domain diam (nm)		no. of molecules per micelle × 10 <sup>-3</sup>	
	φ <sub>cPEO</sub>	φ <sub>hPEO</sub>	obsd	calcd	cPEO	hPEO
1-1	1	0	20-40	45	1.3	0
80/20/0						
2-1	0.492	0.507	20-60	60	1.4	11
87.6/10/2.4						
3-1	0.250	0.750	50-200			
91.5/5/3.5						
4-1	0.165	0.835	50-500			
92.8/3.3/3.9						
5-1	0.074	0.926	150-1000			
94.1/1.5/4.4						

be generalized without difficulty.

The main parts of the paper are sections 3 and 4. In the first of these, we summarize the theory of copolymer micelles in binary copolymer/homopolymer blends, making it explicit simplifications for the strong segregation regime, and then compare its predictions with our experimental results on PS-*b*-PEO micelles in PS. In section 4, we extend the simplified model to ternary systems and again present our experimental results, with comparison. The final section is a brief summary.

## 2. Experimental Section

**2.1. Materials.** Poly(styrene-*block*-ethylene oxide) (PS-*b*-PEO) was prepared by living anionic polymerization in tetrahydrofuran, using a procedure analogous to that employed by O'Malley and Marchessault.<sup>15</sup> Two block copolymers have been used in the micrographic studies of the present work. In each, the molecular weights of the polystyrene blocks were evaluated by gel permeation chromatography, and the molar compositions of the block copolymers were determined by <sup>1</sup>H NMR. The first PS-*b*-PEO copolymer had a molar composition of (59.3/40.7), corresponding number-average block molecular weights of (87K-*b*-27K), and degrees of polymerization  $Z_{cPS} \approx 835$  and  $Z_{cPEO} \approx 600$ . The second had a molar composition of (77.4/22.6), block molecular weights of (84K-*b*-10K), and degrees of polymerization  $Z_{cPS} \approx 810$  and  $Z_{cPEO} \approx 235$ . The polydispersity of the PS blocks was 1.3.

The polystyrene employed as the matrix in all composites was a polystyrene standard (lot no. 61126) obtained from Pressure Chemical (Pittsburgh, PA). The manufacturer reports its number-average molecular weight,  $\bar{M}_n$ , to be 105 000 and a MWD of 1.04. The poly(ethylene oxide) homopolymer employed in this study was poly(ethylene glycol),  $\bar{M}_n = 3400$ , and was obtained from Aldrich Chemical Co. The corresponding degrees of polymerization of these homopolymers are  $Z_{hPS} \approx 1000$  and  $Z_{hPEO} \approx 80$ .

**2.2. Sample Preparation.** Films, approximately 50 μm in thickness, were puddle cast onto glass substrates from a mixed solvent (toluene/tetrahydrofuran/methanol) with composition (85/10/5) by volume. The concentrations of the solutions were approximately 12% solids by weight; the compositions studied are specified in Table 1. The glass substrates were warmed on an aluminum block during film formation to prevent crystallization of PEO prior to solidification of the PS matrix. Dried films were annealed at 120 °C for 16 h prior to TEM. The procedure was designed to ensure that the morphologies were characteristic of amorphous polymers, forming prior to any crystallization.

**2.3. Microscopy.** The films were embedded in an ambient temperature curing two-part epoxy (Araldite 6020, resin/Ancamide 503 hardener) and oven cured at 32 °C for approximately 24 h. The embedded samples were sectioned on a Reichert-Jung Ultracut E microtome. The sections were cut at a 4° tilt. The thin sections were floated on distilled water and collected on 3 mm carbon-coated 200 mesh copper grids. The PEO domains in the sectioned films were then stained selectively by placing a drop of phosphotungstic acid solution (1% by weight)

directly on the grids. After 30 s, the phosphotungstic acid solution was wicked away with a piece of filter paper. The grids were then examined using a Philips CM 12 transmission electron microscope operated at an accelerating voltage of 60 kV.

Representative photomicrographs were taken at magnifications of 5K, 10K, 20K, 50K, 105K, 300K, and 600K. In the present paper, sections from illustrative photomicrographs at magnifications of 5-50K are shown (Figures 4a-c and 7). The data in Table 1 were obtained from the micrographs of greater magnification because only in these micrographs can one accurately measure domain size.

Because of the relative softness of the PS/PS-*b*-PEO and PS/PS-*b*-PEO/PEO composite films, the thin sections were very susceptible to damage. Indeed, in nearly all of the micrographs, one can observe knife marks (striations) in the microtome direction and periodic compression and knife chatter folds which accept stain and produce linear discolorations perpendicular to the microtome direction. In some of the micrographs water has dissolved out PEO, leaving holes where a stained PEO domain would have otherwise been. Accordingly, one observes both white and dark spherical regions distributed more or less uniformly in the sectioned thin films. In the compositions with the highest homopoly(ethylene oxide) content, damage and artifacts are most pronounced. In these micrographs, particularly those for samples 4-1 and 5-1, one also observes tearing and stained spheres of PEO complexed with phosphotungstic acid sitting in larger holes.

## 3. Binary Copolymer/Homopolymer Mixtures

**3.1. System Description.** The generic binary system of interest consists of homopolymer, which we label hA, and A-*b*-B block copolymer with one of the blocks corresponding to the homopolymer. We denote the degree of polymerization of the homopolymer by  $Z_{hA}$ , those of the two blocks of the copolymer by  $Z_{cA}$  and  $Z_{cB}$ , and the total for the block copolymer by  $Z_C = Z_{cA} + Z_{cB}$ . It is assumed that all A-B interactions can be modeled by a single Flory parameter  $\chi$ , irrespective of whether the monomers belong to copolymers or homopolymers. The majority component is the homopolymer, which typically comprises 80% or more of the composition. The overall volume fractions of each component are denoted by  $\phi_{hA}$  and  $\phi_C$ , and the overall volume fractions of A and B due to the block copolymer by  $\phi_{cA}$  and  $\phi_{cB}$ . These are related to  $\phi_C$  by

$$\phi_{c\kappa} = f_{\kappa} \phi_C \quad (3.1)$$

for  $\kappa = A, B$ , where  $f_{\kappa}$  is the volume fraction of block  $\kappa$  of the copolymer. They satisfy  $f_A + f_B = 1$  and are given by

$$f_{\kappa} = \frac{Z_{c\kappa} \rho_{0C}}{Z_C \rho_{0\kappa}} \quad (3.2)$$

where each  $\rho_{0\kappa}$  is the monomer number density of a system consisting of pure component  $\kappa$  and  $\rho_{0C}$  is a weighted average of these, given by

$$Z_C / \rho_{0C} = Z_{cA} / \rho_{0A} + Z_{cB} / \rho_{0B} \quad (3.3)$$

**3.2. Theory.** We begin the theoretical analysis with a summary of the assumptions and results of the existing model for binary A-*b*-B/hA copolymer/homopolymer systems.<sup>2</sup> The first point to note is that it describes systems which are at least in metastable equilibrium; the overall approach consists of developing an approximate expression for the free energy of the micellar system and finding a local minimum of that expression.

The expression for the free energy is based on the simple physical model illustrated in Figure 1. The system is assumed to consist of identical, spherical micelles randomly

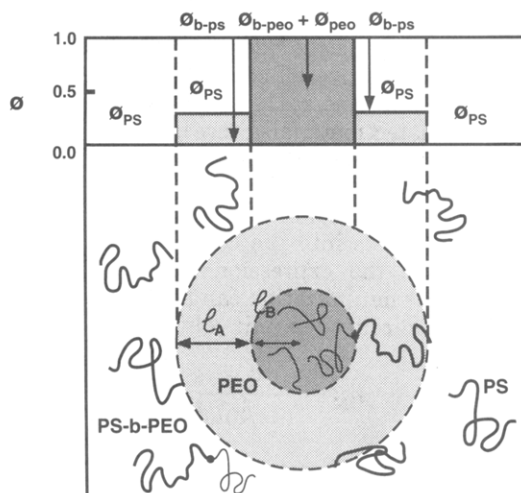


**Figure 1.** Schematic picture of the swollen micelle system. The core region, with radius denoted  $l_B$ , is assumed to consist of the B block of the copolymer and, in the swollen micelle case, B homopolymer. The corona consists of the A block of the copolymer and A homopolymer, with thickness denoted  $l_A$ . The host material outside the micelles is A homopolymer. There is also some copolymer remaining in the host matrix; its volume fraction defines the critical micelle concentration. It is assumed that the volume fraction of the B homopolymer in the matrix is negligible. The system studied experimentally in this paper corresponds to B  $\equiv$  PEO and A  $\equiv$  PS.

dispersed throughout an otherwise homogeneous matrix. Each micelle is modeled as a spherical core of radius  $l_B$ , surrounded by a corona of thickness  $l_A$ . Thus there are three distinct types of regions: region 1 consists of the micelle cores, region 2 the coronas, and region 3 the matrix. We also assume the density of micelles to be sufficiently low that their mutual interactions are negligible.

To obtain a relatively simple expression for the free energy, the density of each component is assumed to be constant throughout each of the three types of regions. Block copolymer molecules can be found in either micelles or the matrix, with the fractions of block copolymers in these regions denoted by  $F_M^C$  and  $F_3^C = 1 - F_M^C$ , respectively. It is assumed that any block copolymer molecule which is in a micelle has its joint located within the narrow interface at the core–corona interface, with the cB block extending inward into the core and the cA block extending outward into the corona. Block copolymer remaining in solution is treated as Gaussian. Homopolymer, hA, can be found in any of the three regions. Denoting the local volume fraction of component  $\kappa$  in region  $i$  by  $\phi_\kappa^{(i)}$ , then incompressibility implies

$$\phi_{cB}^{(1)} + \phi_{hA}^{(1)} = 1 \quad (3.4)$$

$$\phi_{cA}^{(2)} + \phi_{hA}^{(2)} = 1 \quad (3.5)$$

$$\phi_C^{(3)} + \phi_{hA}^{(3)} = 1 \quad (3.6)$$

It is convenient to work with the free energy of the system with micelles,  $G_M$ , relative to that of a homogeneous system in which all the block copolymer remains in solution in the matrix,  $G_H$ , and to express it as the free energy per unit volume, in units of  $k_B T \rho_0$ , where  $k_B$  is the Boltzmann constant,  $T$  is the temperature, and  $\rho_0$  is any convenient reference density:

$$\Delta g = \frac{G_M - G_H}{\rho_0 k_B T V} \quad (3.7)$$

In this paper we take  $\rho_0$  to be the geometric mean of  $\rho_{0A}$  and  $\rho_{0B}$ .

We approximate  $\Delta g$  by the sum of six terms, discussed below, which depend on the local volume fractions of each component in each region, the relative size of each region, the number density of micelles,  $n_M$ , and the fraction of copolymer and homopolymer in each region. This expression must then be minimized with respect to the independent variables, which can be taken to be  $l_B$ ,  $l_A$ ,  $n_M$ , and  $F_M^C$ .

One of the results of the calculations presented in ref 2 is that, for block copolymer/homopolymer blends, the volume fraction of matrix homopolymer in the core is very low,  $\phi_{hA}^{(1)} \lesssim 0.02$  in virtually all cases. For this reason, in the rest of this paper we neglect penetration of the micelle cores by the incompatible, matrix homopolymer and consider the simplified version of the theory that results.

Of the six contributions to the free energy, the largest individual one is the change in the interaction energy, i.e., the reduction in free energy due to the reduced A–B contacts in the micelle phase as compared with the homogeneous phase. This can be expressed

$$\Delta g_{\text{int}} = -\chi \phi_{cB} \left[ \phi_{cA} \left( 1 - \frac{(F_3^C)^2}{G_3^v} \right) + \phi_{hA} \left( 1 - \frac{F_3^C F_3^{hA}}{G_3^v} \right) \right] \quad (3.8)$$

In this expression,  $G_i^v$  is the fraction of the total volume occupied by region  $i$ ,  $i = 1, 2$ , and 3, and  $F_i^{hA}$  is the fraction of hA in region  $i$ .

There is an interface at each core–corona boundary, with an interfacial tension denoted  $\gamma$ . The interfacial energy per unit volume of the system can be approximated by

$$\Delta g_I = \frac{\gamma}{\rho_{0R} k_B T V} A \quad (3.9)$$

where  $A$  is the total interfacial area,  $A = N_M (4\pi l_B^2)$ , and  $N_M$  is the total number of micelles. The number density of micelles is  $n_M = N_M/V$ . For the interfacial tension, we use the approximate expression

$$\frac{\gamma}{\rho_{0R} k_B T} \simeq (\chi/6)^{1/2} b \quad (3.10)$$

where  $b$  is an average Kuhn length and  $\rho_{0R}$  is a reference density. In the analysis leading to eq 3.10, it was assumed that the pure component densities are equal, as are the Kuhn lengths. For most systems, such as PS/PEO, this is not the case. In this paper we use  $\rho_{0R} = \rho_0$ , as in eq 3.7, and  $b = (b_A b_B)^{1/2}$ , recognizing that such choices have quantitative effects. Combining eqs 3.9 and 3.10 yields

$$\Delta g_I \simeq (\chi/6)^{1/2} n_M (4\pi l_B^2) b \quad (3.11)$$

The same analysis gave the following expression for the width of the interface,  $d$ ,

$$d \simeq \left( \frac{2}{3\chi} \right)^{1/2} b \quad (3.12)$$

The existence of the micelles implies that the molecules are at least partially segregated between the regions. Those block copolymer molecules which are localized to micelles have their A–B joints in the interfacial regions, which occupy a total volume  $Ad$ . The remaining copolymer is expelled from the micelles into the matrix whose relative volume fraction is  $G_3^v$ . The associated change in entropy leads to an increase in free energy of

$$\Delta g_j \simeq \frac{\rho_{0C} \phi_C}{\rho_0 Z_C} \left[ F_M^C \ln \left( \frac{F_M^C}{n_M (4\pi l_B^2) d} \right) + F_3^C \ln \left( \frac{F_3^C}{G_3^v} \right) \right] \quad (3.13)$$

Similarly, the restriction of the hA to regions 2 and 3 gives a contribution

$$\Delta g_h \simeq \frac{\rho_{0A} \phi_{hA}}{\rho_0 Z_{hA}} \left[ F_2^{hA} \ln \left( \frac{F_2^{hA}}{G_2^v} \right) + F_3^{hA} \ln \left( \frac{F_3^{hA}}{G_3^v} \right) \right] \quad (3.14)$$

Of itself, the existence of the interfacial energy tends to induce large micelles, since this would be accompanied by a reduction in the number of micelles and total interfacial area. However, the micelle centers are not empty, the cB blocks stretch into the micelle centers, and this stretching results in a reduction in entropy. In addition, hA penetrates into the coronas for entropic reasons, and this causes a stretching of the cA copolymer blocks. The associated elastic free energy is approximated by

$$\Delta g_{el} \simeq \frac{\rho_{0C} \phi_C}{\rho_0 Z_C} \frac{F_M^C}{2} \left( \alpha_B^2 + \frac{2}{\alpha_B} + \alpha_A^2 + \frac{2}{\alpha_A} - 6 \right) \quad (3.15)$$

where each  $\alpha_k$  is a measure of the stretching of the corresponding block in one direction relative to its root mean squared end-to-end value. They are approximated by

$$\alpha_k \simeq \left( \frac{3}{Z_{ck}} \right)^{1/2} \frac{l_k}{b_k} \quad (3.16)$$

The final contribution to the free energy is due to the translational entropy of the micelles themselves. However, it is 2–3 orders of magnitude smaller than the other contributions, and so we ignore it in this paper. The final expression for  $\Delta g$  used as the basis for the current paper is obtained by summing eqs 3.8, 3.11, and 3.13–3.15.

In ref 2, the calculation of the system properties used the numerical minimization of the expression for  $\Delta g$ . The cmc, which is defined as the block copolymer concentration remaining in solution when micelles are present, was found to be very sensitive to the product  $\chi Z_{cB}$ , decreasing approximately exponentially with it. In contrast, it increases slowly with increasing  $Z_{cA}$ . Finally, it is a decreasing function of  $Z_{hA}$ , although this is also a weak dependence.

For the characteristics of the micelles themselves, the results for  $l_B$  and  $l_A$  can be summarized approximately by

$$l_B \propto Z_{cA}^\mu Z_{cB}^\nu \quad (3.17)$$

$$l_A \propto Z_{cA}^\omega \quad (3.18)$$

where the exponents were somewhat variable but fell within the ranges

$$\begin{aligned} \mu &\lesssim 0 \\ \frac{2}{3} &\lesssim \nu \lesssim \frac{3}{4} \\ \frac{1}{2} &\lesssim \omega \lesssim 1 \end{aligned} \quad (3.19)$$

The meaning of these results is that the core radius depends primarily on the degree of polymerization of the copolymer block forming the core, increasing with  $Z_{cB}$ , but that it decreases slightly as  $Z_{cA}$  increases. As discussed

further below, the corona thickness corresponds to unstretched ( $\omega = 1/2$ ) or stretched ( $\omega > 1/2$ ) cA blocks.

In many cases, the overall copolymer concentration is much larger than the cmc, so that only a very small fraction remains in the matrix material. Since the hA homopolymer concentration in the cores is also very small, it is useful to introduce the limiting case in which *all* the copolymer is assumed to form micelles and *none* of the hA homopolymer to penetrate into the cores. For this strongly segregated limit, the expression for the free energy simplifies and its minimization can be done analytically. The number of micelles per unit volume becomes simply

$$n_M \rightarrow \frac{\phi_{cB}}{(4\pi/3) l_B^3} \quad (3.20)$$

and the free energy reduces to

$$\begin{aligned} \Delta g \rightarrow & -\chi \phi_{cB} (\phi_{cA} + \phi_{hA}) + \\ & \left( \frac{3\chi}{2} \right)^{1/2} \phi_{cB} \left( \frac{b}{l_B} \right) + \frac{\rho_{0C} \phi_C}{\rho_0 Z_C} \ln \left( \frac{l_B}{3d} \frac{1}{\phi_{cB}} \right) + \\ & \frac{1}{2} \frac{\rho_{0C} \phi_C}{\rho_0 Z_C} \left( \alpha_B^2 + \frac{2}{\alpha_B} + \alpha_A^2 + \frac{2}{\alpha_A} - 6 \right) + \\ & \frac{\rho_{0A} \phi_{hA}}{\rho_0 Z_{hA}} \left[ F_2^{hA} \ln \left( \frac{F_2^{hA}}{G_2^v} \right) + F_3^{hA} \ln \left( \frac{F_3^{hA}}{G_3^v} \right) \right] \end{aligned} \quad (3.21)$$

This expression facilitates the identification of the factors which primarily control various properties. First, only the second, third, and fourth terms of eq 3.21 depend explicitly on the core radius, and it is the second and fourth terms which are of primary importance. Physically, this means that the micelle core sizes are determined predominantly by the balance between the stretching of the cB copolymer blocks and the interfacial tension at the core/corona interface. Minimizing these contributions with respect to  $l_B$  yields a simple expression which can be solved analytically as long as  $\alpha_B \gg 1$ , which is frequently the case. This yields<sup>16</sup>

$$l_B \simeq \left( \frac{\chi}{6} \right)^{1/6} \left( \frac{\rho_0}{\rho_{0B}} \right)^{1/3} Z_{cB}^{2/3} (bb_B^2)^{1/3} \quad (3.22)$$

which usually agrees with the result of a numerical minimization of the free energy to within a few percent.

The corona thickness,  $l_A$ , is determined primarily by the last two terms in  $\Delta g$ , i.e., the stretching of the cA block and the partial expulsion of the host homopolymer from the micelles. In the limit of very large  $Z_{hA}$  the entropic effects due to the expulsion of the homopolymer become negligible, the stretching term dominates, and  $\Delta g$  is minimized by  $\alpha_A \simeq 1$ . Hence

$$l_A \simeq \left( \frac{Z_{cA}}{3} \right)^{1/2} b_A \quad (3.23)$$

Equations 3.22 and 3.23 agree with the one limit for the values of the exponents as given in eq 3.19. The relatively small deviations from these values are due to the other terms in the free energy. In particular, for finite  $Z_{hA}$ , the penetration of the homopolymer into the coronas induces stretching of the cA copolymer blocks, increasing the corresponding power to  $\omega > 1/2$ . This is accompanied by a small reduction of the core radius, i.e.  $\mu \lesssim 0$ . Since this effect is due to the entropy of the homopolymer, it increases with decreasing  $Z_{hA}$ .

The number density of micelles and the number of copolymer molecules per micelle are easily calculated in this limit. Combining eqs 3.20 and 3.22 gives

$$n_M = \left( \frac{27}{8\pi^2\chi} \right)^{1/2} \left( \frac{\rho_{0B}}{\rho_0 b b_B^2} \right) \frac{\phi_{cB}}{Z_{cB}^2} \quad (3.24)$$

Likewise, combining eq 3.22 with the volume per cB block gives

$$N_C \simeq \left( \frac{8\pi^2\chi}{27} \right)^{1/2} (\rho_0 b b_B^2) Z_{cB} \quad (3.25)$$

for the number of copolymers per micelle.

A full understanding of the factors controlling the cmc requires the numerical minimization of the free energy. However, a leading order approximation can be obtained by noting that the two most important terms in this regard are the reduction in the interaction energy, which favors micelle formation, and the copolymer localization term, which opposes it. If we were to approximate the cmc as the copolymer volume fraction at which these two terms balance and use eq 3.22 for  $l_B$ , this would give

$$\phi_C^{\text{crit}} \simeq \left( \frac{\chi Z_{cB}}{6} \right)^{2/3} \frac{1}{f_B} e^{-(\rho_0/\rho_{0B})\chi Z_{cB}} \quad (3.26)$$

for the cmc. This illustrates that the strong dependence of the cmc on  $\chi Z_{cB}$  results from the balance between the enthalpy and the localization of the copolymer. However, eq 3.26 is by no means quantitative; the approach neglects the fact that some copolymer remains in solution, and neglected terms in the free energy appear in the argument of the exponential in eq 3.26 and can have a very significant effect.

To summarize, eqs 3.22–3.26 exhibit the primary physical results of the model. First, the cmc depends very strongly on  $\chi Z_{cB}$  and weakly on  $Z_{cA}$  and  $Z_{hA}$ . This dependence on  $\chi Z_{cB}$  manifests itself as a dramatic threshold dependence on the degree of polymerization of the B block of the copolymer. As long as  $\phi_C$  exceeds the cmc, micelles form with core radii which are nearly independent of  $\phi_C$ , depending primarily on  $Z_{cB}$  and weakly on temperature,  $l_B \propto \chi^{1/6} Z_{cB}^{2/3}$ . The number of molecules per micelle depends on the same variables. The number of micelles per unit volume is determined by  $Z_{cB}$ , the overall cB volume fraction, and  $\chi$ . It should also be noted that the dependence of each of these characteristics on the cA block is the opposite of that on the cB block. For example, the cmc decreases with increasing  $Z_{cB}$  but increases with increasing  $Z_{cA}$ .

**3.3. The PS/PS-*b*-PEO System: Theory and Experiment.** The threshold type dependence of the cmc on  $\chi Z_{cB}$  can be illustrated by calculating the fraction of chains in micelles as a function of  $Z_{cB}$  for a given value of  $\chi$ . Figure 2, which was calculated from the numerical minimization of the full free energy expression, shows this fraction for PS/PS-*b*-PEO binary blends in which the overall copolymer volume fraction was maintained at 10%.

For this figure, the degree of polymerization of the polystyrene host is 400, that of the PS block of the block copolymer is  $Z_{cPS} = 600$ , while that of the PEO block,  $Z_{cPEO}$ , is varied. The reference densities and Kuhn lengths were taken from the literature, i.e.,  $\rho_{PEO} = 16.9 \text{ nm}^{-3}$ ,  $\rho_{PS} = 6.3 \text{ nm}^{-3}$ ,  $b_{PEO} = 0.5 \text{ nm}$ , and  $b_{PS} = 0.7 \text{ nm}$ ,<sup>17</sup> and three different values of  $\chi$ , 0.8, 0.5, and 0.2, were investigated.

DiPaoli-Baranyi and Van Laeken et al. evaluated  $\chi$  for PS-PEO block copolymers in the melt at 150 °C using inverse gas chromatography.<sup>18</sup> They obtained values ranging from 0.27 to 0.4 with an average of about 0.3,<sup>19</sup> which is consistent with earlier measurements of  $\chi \simeq 0.28$  by Nagata et al.<sup>22</sup> In the rest of this paper, we assume a value of  $\chi \simeq 0.3$  is reasonable for PS-PEO.

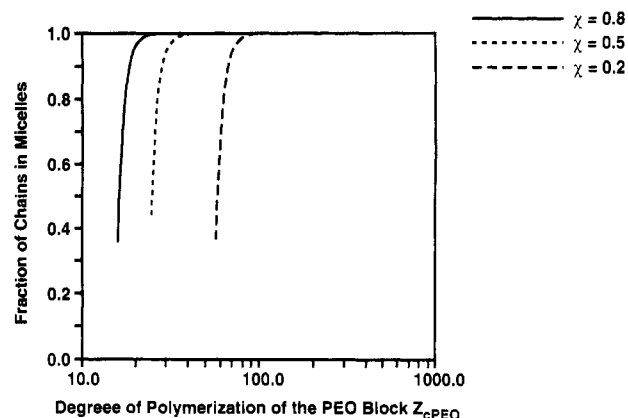


**Figure 2.** Calculated fraction of copolymer molecules which aggregate into micelles in a binary PS-*b*-PEO/PEO mixture as a function of  $Z_{cPEO}$ . The calculations were done assuming an overall copolymer volume fraction  $\phi_C = 0.1$ , using degrees of polymerization  $Z_{cPS} = 600$  and  $Z_{hPS} = 400$ , and using literature values of the pure component densities and Kuhn lengths. Each curve corresponds to a different assumed value of  $\chi$ , as indicated. Below values of about 0.4, this fraction falls rapidly to zero as  $Z_{cPEO}$  decreases.

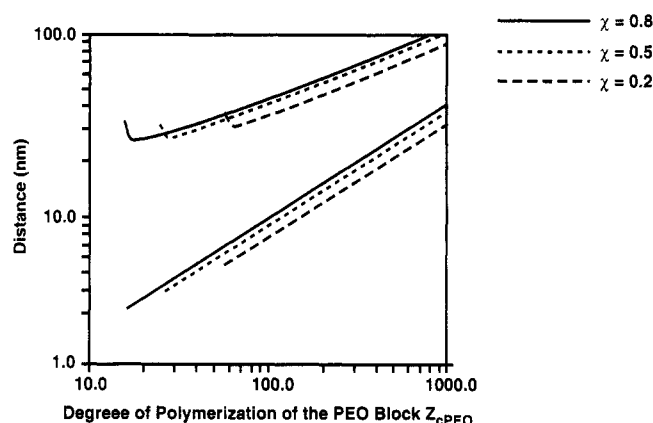


**Figure 3.** Calculated values of the micelle core radius  $l_B$  (lower three curves) and average unit cell radius  $R$  (upper three curves) for the same system as in Figure 2. The average unit cell radius is the radius of a sphere which, on average, contains one micelle, and so is directly related to the number density of micelles. The lower end of each curve corresponds to the value of  $Z_{cPEO}$  at which the fraction of copolymer forming micelles falls to zero, as on Figure 2. Except near this regime, the curves are well described by eqs 3.22 and 3.24.

Although the results of Figure 2 are for the specific systems, their nature is quite general. For  $Z_{cPEO}$  below a certain value, the fraction of copolymer in micelles is essentially zero. Once a certain threshold is reached, then, as a function of  $Z_{cPEO}$ , this fraction rises rapidly, essentially to unity. The threshold value of  $Z_{cPEO}$  is, approximately, inversely proportional to  $\chi$ ; for  $\chi = 0.3$ , it is on the order of  $Z_{cPEO} \simeq 100$ . Thus, this model predicts that micelles should not form in binary mixtures of a block copolymer of polystyrene and poly(ethylene oxide) in which the degree of polymerization of the PEO block is much less than about 100.

As long as  $\phi_C$  exceeds  $\phi_C^{\text{crit}}$ , the theory predicts that the core radius of the micelles which form,  $l_B$ , is relatively independent of  $\phi_C$  and determined primarily by  $Z_{cB}$ . This functional dependence is illustrated by the three lower curves of Figure 3, which show the core radius of PS-*b*-PEO micelles as a function of  $Z_{cPEO}$ , using the same values of  $Z_{hPS}$ ,  $Z_{cPS}$ , and  $\chi$  as in Figure 2. It is well described by eq 3.22.

The three upper curves in Figure 3 show the average unit cell radius, denoted  $R$ , for this system. It is defined



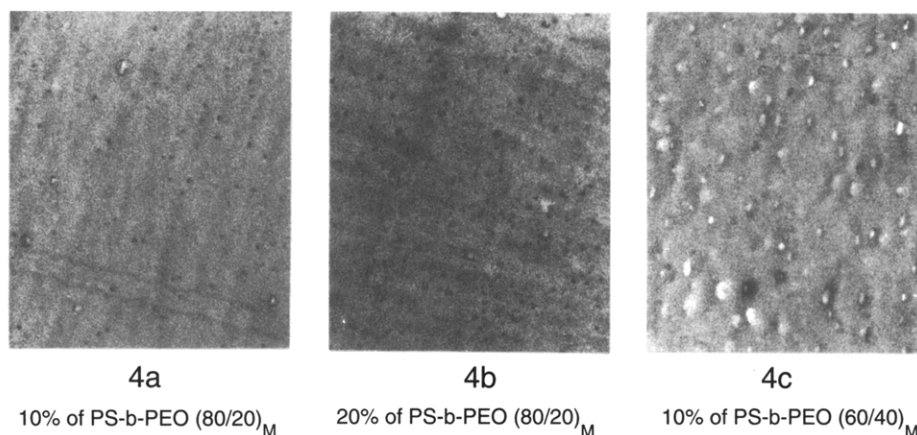


**Figure 4.** Illustrative micrographs for thermally annealed composites of 10% (a) and 20% (b) by weight of PS-*b*-PEO(77.4/22.6)<sub>M</sub> in PS and 10% (c) by weight of PS-*b*-PEO(59.3/40.7)<sub>M</sub> in PS stained with phosphotungstic acid.

as the radius of a sphere which, on average, contains one micelle and is related to the number density of micelles by

$$n_m = (4/3\pi R^3)^{-1} \quad (3.27)$$

The specific dependence of  $R$  on  $Z_{cB}$  illustrated in Figure 3 is due, in part, to the fact that the overall copolymer volume fraction was held fixed. As a consequence, both the core radius and  $\phi_{cB}$  vary with  $Z_{cB}$ . Neglecting the differences in reference densities, the result is that, in the strong segregation limit where virtually all copolymers are in micelles,  $R$  scales approximately as

$$R \simeq \left(\frac{\chi}{6}\right)^{1/6} \left(\frac{Z_c Z_{cB}}{\phi_c}\right)^{1/3} (bb_B^2)^{1/3} \quad (3.28)$$

This is consistent with the curves of Figure 3, except near the lower end of each of them where the copolymer fraction in micelles begins to fall to zero. In this regime, as  $Z_{cB}$  decreases, so does this fraction, and so the average distance between micelles increases. The result is the upturn in each of these curves near their termination at low  $Z_{cB}$ .

We have synthesized block copolymers in which the degree of polymerization of the PS block was varied between 480 and 960, and the percent PEO in the molecules between 3% and 45% by weight. In PS/PS-*b*-PEO blends using block copolymers with PS block molecular weights ranging from 50 000 to 80 000 and containing low percentages of PEO (3–7% by weight) we did not observe micellization of the block copolymer in transmission electron micrographs stained with phosphotungstic acid, while micelles did tend to form for copolymers with larger  $Z_{cPEO}$ . These observations are consistent with the model prediction of an approximately threshold type behavior occurring near  $Z_{cPEO} \simeq 100$ .

Figure 4 shows a set of micrographs for the two block copolymers that were used in the micrographic studies in the present work, which were prepared and analyzed as described in section 2. They are for thermally annealed composites of 10% (Figure 4a) and 20% (Figure 4b) by weight of PS-*b*-PEO(77.4/22.6)<sub>M</sub> in PS and 10% (Figure 4c) by weight of PS-*b*-PEO(59.3/40.7)<sub>M</sub> in PS. Since  $Z_{cPEO}$  exceeds the threshold value of 100 by factors of about 6 and 2, respectively, the theory predicts that virtually all copolymer is in micelles in these systems.

Micrograph 4a is a microtomed section stained with phosphotungstic acid and shows a low areal density of PEO micelle cores from the (77.4/22.6)<sub>M</sub> block copolymer, randomly distributed in a PS continuum. The core radii range in size from 10 to 20 nm. Micrograph 4b is for 20%

of the same block copolymer in PS. Here one observes a dramatically increased areal density of PEO micelle cores randomly distributed in the PS host. The range of size of core radii remains unchanged, consistent with the theoretical result that the volume fraction of PS-*b*-PEO in the PS host has little effect on the micelle size. Micrograph 4c is a microtomed section stained with phosphotungstic acid for 10% of PS-*b*-PEO(59.3/40.7)<sub>M</sub> in PS. In this sample, the core radii range from 20 to 40 nm. Core radii calculated for the two block copolymers used in Figure 4a–c are 20 and 40 nm, respectively. Given that the nonequilibrium micelle sizes may be smaller than those at equilibrium, the theoretical results are consistent with the core sizes measured in the transmission electron micrographs of this figure.

#### 4. Ternary Mixtures

**4.1. System Description.** We turn now to extending the model described above to mixtures in which hB homopolymer is added in an attempt to swell the micelle cores. The generic system now consists of the binary system described in section 3.1, plus hB homopolymer of degree of polymerization  $Z_{hB}$  and overall volume fraction  $\phi_{hB}$ . All A–B interactions are modeled by one Flory parameter  $\chi$ . The total volume fraction of B polymer is  $\phi_B = \phi_{cB} + \phi_{hB}$ .

These blends can, in principle, exhibit a number of morphologies. For the systems of interest in this paper,  $\phi_{hA} \gtrsim 0.8$ , the possibilities we consider are a single homogeneous macrophase, a single macrophase but populated by micelles whose sizes are on the order of molecular dimensions, or macrophase-separated systems. These generally consist of micron-sized or larger domains within the overall hA matrix.

**4.2. Theory.** Restricting attention to systems such as those studied experimentally above in the regime of strong segregation, i.e.,  $Z_{cB}$  well above the threshold value for micelle formation, we assume here that virtually all block copolymer is in micelles and that there is no hA homopolymer in the cores. Furthermore, we limit consideration to systems in which the homopolymers are incompatible, so the concentration of hB within the matrix hA is negligible. Thus, hB homopolymer is assumed either to be solubilized within swollen micelle cores or to be expelled into a second macrophase. In practice, this second phase consists of domains which are of no fixed size but are generally on the order of microns.

We formulate the problem by developing an expression for the free energy of the system as a function of the fraction of the hB homopolymer solubilized within the micelle cores,

which we denote  $f$ , and then calculating the equilibrium value of  $f$  by minimizing the free energy. The fraction of the volume of the entire system which consists of micelle cores is now

$$\phi_{\text{core}} = \phi_{\text{cB}} + f\phi_{\text{hB}} \quad (4.1)$$

and the fraction occupied by the separate hB phase is  $(1 - f)\phi_{\text{hB}}$ . In analogy with eq 3.24, the total number of micelles divided by the total volume, including the volume occupied by any phase-separated polymer, is

$$n_{\text{M}} = \frac{3}{4\pi l_{\text{B}}^3} \phi_{\text{core}} \quad (4.2)$$

where  $l_{\text{B}}$  is the radius of each micelle in the ternary system.

An important assumption underlying our picture of swollen micelles is that the hB homopolymer which is solubilized is distributed throughout the cores. This is justified in part by the fact that we restrict our consideration to hB homopolymer with degree of polymerization less than that of the corresponding cB block. For these cases, there has accumulated both experimental<sup>23-26</sup> and theoretical<sup>10,27</sup> evidence that, because of entropy of mixing effects, solubilized homopolymer is distributed throughout the subdomains. (The picture is more complicated if  $Z_{\text{hB}} \gtrsim Z_{\text{cB}}$ .)

For simplicity, we assume that the hB homopolymer is uniformly distributed throughout the cores and consequently that the hB and cB volume fractions are constant in each core, as indicated in Figure 1. This means that the cB blocks are assumed to stretch into the centers of the cores for both the swollen and unswollen micelles. If this were not the case and the copolymer relaxed to a less stretched conformation, homopolymer could accumulate in the centers, and the free energy would be minimized by the formation of few, relatively very large domains. However, this would be the macrophase-separated system, with surfaces decorated by copolymer. The model we develop here considers the two limits of the above picture: swollen micelles with uniform cores, and macrophase-separated hB homopolymer.

The expression for the free energy is based on generalizing the five terms of eq 3.21, the first of which is the interaction term. Since we assume that the hB homopolymer is segregated into either the cores or the second phase, there is no bulk A-B mixing in either case, and this interaction term is independent of the fraction  $f$ .

Both the interfacial free energy and copolymer localization terms depend on  $f$  through changes in the core volume fractions. Hence, the expressions for  $\Delta g_{\text{I}}$  and  $\Delta g_{\text{J}}$  can be obtained from the corresponding ones for the binary system via the simple replacement of  $\phi_{\text{cB}}$  with  $\phi_{\text{core}}$ .

For  $\Delta g_{\text{h}}$ , we first make the simplification of neglecting any effect of core swelling on the volume of the corona and hence assume that the contribution of the hA homopolymer to  $\Delta g$  is independent of  $f$ .<sup>28</sup> Next, we note that  $f = 0$  corresponds to all the hB homopolymer being demixed into a separate phase of volume fraction  $\phi_{\text{hB}}$ . On the other hand, if  $f = 1$  then these homopolymer molecules can occupy a larger volume fraction,  $\phi_{\text{B}} = \phi_{\text{cB}} + \phi_{\text{hB}}$ , and therefore have greater entropy. For  $0 < f < 1$ , a fraction  $f$  is localized to a relative volume  $\phi_{\text{core}}$ , and the remaining fraction  $1 - f$  to a relative volume  $(1 - f)\phi_{\text{hB}}$ . The  $f$ -dependent part of the free energy due to the homopolymer can be expressed

$$\Delta g_{\text{h}} \simeq \frac{\rho_{\text{0B}}}{\rho_0} \frac{\phi_{\text{hB}}}{Z_{\text{hB}}} \left[ f \ln \left( \frac{\phi_{\text{B}}}{\phi_{\text{core}}} \right) + (1 - f) \ln \left( \frac{\phi_{\text{B}}}{(1 - f)\phi_{\text{hB}}} \right) \right] \quad (4.3)$$

Finally, we need the elastic free energy. As discussed above, we approximate the stretching free energy of the cB blocks by assuming that they extend to the centers. Hence,  $\Delta g_{\text{el}}$  is again given by eq 3.15. For simplicity, we also neglect any changes in stretching of the corona blocks due to core swelling.

Summing the resulting expressions for the individual contributions to the free energy gives our approximate  $\Delta g$  as a function of  $f$ . It is convenient to subtract a constant, which we take to be the free energy of the system with the hB fully demixed. An additional simplification can be made by using eqs 3.1 and 3.2 to eliminate  $\phi_{\text{C}}$  in favor of  $\phi_{\text{cB}}$ , resulting in

$$\begin{aligned} \Delta \tilde{g} \equiv \Delta g(f) - \Delta g(f=0) \\ = \left( \frac{3\chi}{2} \right)^{1/2} \left( \frac{\phi_{\text{core}} b}{l_{\text{B}}} - \frac{\phi_{\text{cB}} b}{l_{\text{B}}^0} \right) + \frac{\rho_{\text{0B}}}{\rho_0} \left\{ \frac{\phi_{\text{cB}}}{Z_{\text{cB}}} \left[ \ln \left( \frac{l_{\text{B}}}{\phi_{\text{core}}} \frac{\phi_{\text{cB}}}{l_{\text{B}}^0} \right) + \frac{1}{2} \left( \alpha_{\text{B}}^2 + \frac{2}{\alpha_{\text{B}}} - (\alpha_{\text{B}}^0)^2 - \frac{2}{\alpha_{\text{B}}^0} \right) \right] + \frac{\phi_{\text{hB}}}{Z_{\text{hB}}} \left[ f \ln \left( \frac{\phi_{\text{hB}}}{\phi_{\text{core}}} \right) - (1 - f) \ln(1 - f) \right] \right\} \quad (4.4) \end{aligned}$$

where  $l_{\text{B}}^0$  is the core radius of the unswollen micelles, as calculated in the previous section, eq 3.22. Similarly,  $\alpha_{\text{B}}^0$  is the associated stretching of the cB block.

Equation 4.4 is the basis for the theoretical results discussed in the rest of this paper. The calculation of the properties of the ternary system requires the minimization of this expression with respect to the independent variables, which are  $l_{\text{B}}$  and  $f$ .

As for the binary copolymer/homopolymer blends discussed in the previous section, the dominant factor controlling the core radius is the balance of the elastic and interfacial free energies. Minimizing the free energy with respect to  $l_{\text{B}}$  and assuming, as before, that  $\alpha_{\text{B}} \gg 1$ , yields

$$l_{\text{B}} \simeq \left( \frac{\phi_{\text{core}}}{\phi_{\text{cB}}} \right)^{1/3} l_{\text{B}}^0 \quad (4.5)$$

where  $l_{\text{B}}^0$  is the unswollen micelle radius. This depends on the fraction of solubilized homopolymer,  $f$ , through  $\phi_{\text{core}}$ .

Substituting this into eq 4.2 yields the total number of micelles per unit volume, which turns out to be unchanged. Thus this model predicts that the fraction of homopolymer that is solubilized results in the swelling of individual micelles but leaves the number of micelles unchanged.

To calculate  $f$ , we next substitute eq 4.5 into eq 4.4, which gives

$$\begin{aligned} \Delta \tilde{g} = \frac{\rho_{\text{0B}}}{\rho_0} \frac{\phi_{\text{cB}}}{Z_{\text{cB}}} \left\{ \left( \frac{9\chi Z_{\text{cB}}}{2} \right)^{1/3} \left( \frac{\rho_0 b}{\rho_{\text{0B}} b_{\text{B}}} \right)^{2/3} \left[ \left( \frac{\phi_{\text{core}}}{\phi_{\text{cB}}} \right)^{2/3} - 1 \right] + \frac{2}{3} \ln \left( \frac{\phi_{\text{cB}}}{\phi_{\text{core}}} \right) + \frac{(\alpha_{\text{B}}^0)^2}{2} \left[ \left( \frac{\phi_{\text{core}}}{\phi_{\text{cB}}} \right)^{2/3} - 1 \right] + \frac{1}{\alpha_{\text{B}}^0} \left[ \left( \frac{\phi_{\text{cB}}}{\phi_{\text{core}}} \right)^{1/3} - 1 \right] + \frac{Z_{\text{cB}}}{Z_{\text{hB}}} \frac{\phi_{\text{hB}}}{\phi_{\text{cB}}} \left[ f \ln \left( \frac{\phi_{\text{hB}}}{\phi_{\text{core}}} \right) - (1 - f) \ln(1 - f) \right] \right\} \quad (4.6) \end{aligned}$$

for the free energy. For a given set of densities  $\rho_{\text{0}\alpha}$ , this is a function of four variables,  $\chi Z_{\text{cB}}$ ,  $Z_{\text{hB}}/Z_{\text{cB}}$ ,  $\phi_{\text{hB}}/\phi_{\text{cB}}$ , and  $f$ . The first three specify the system, and minimizing  $\Delta \tilde{g}$  with respect to  $f$  yields the predicted equilibrium fraction of solubilized hB for that system.

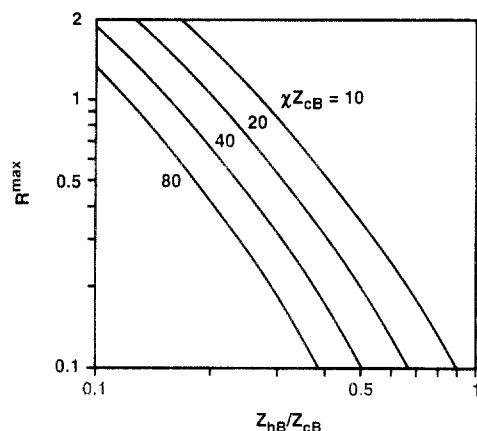


**Figure 5.** Calculated solubility limits of B homopolymer relative to the cB content,  $R^{\max} = \phi_{hB}^{\max}/\phi_{cB}$ , as a function of the relative degrees of polymerization,  $Z_{hB}/Z_{cB}$ , for different values of  $\chi Z_{cB}$  as shown. The system modeled in this figure is one in which the Kuhn statistical lengths are equal, i.e.,  $b_A = b_B$ , as are the two pure component densities,  $\rho_{0A} = \rho_{0B}$ .

This minimization is done numerically, and it turns out that, for the model free energy used here, the equilibrium value of  $f$  is always either zero or 1. This can be understood by considering increasing  $\phi_{hB}$  from zero. Initially, all the homopolymer is solubilized in the cores ( $f = 1$ ) because of entropic effects, even though this is accompanied by small increases in the stretching and interfacial free energies. This occurs because the volume of the (swollen) micelle cores exceeds that of a separate hB phase. However, when a certain threshold is reached, then because of the increases in the free energy due to the stretching and interfacial tension, the homopolymer is expelled into a second phase. If only a fraction of the added homopolymer were expelled, then it would be localized to a correspondingly small fraction of the total volume and have a very low associated entropy. As well, the changes in free energy due to reductions in the stretching and interfacial free energies would be small. Instead, the model predicts that once the threshold is reached, all the homopolymers are expelled from the cores into the second phase of volume fraction  $\phi_{hB}$ , effecting a larger reduction in the stretching and interfacial free energies, and larger entropy of the expelled homopolymers, than would otherwise be the case.

We identify the solubilization limit of the homopolymer as the largest value of  $\phi_{hB}$  for which  $f = 1$ . Labeling this limit  $\phi_{hB}^{\max}$ , the functional form of eq 4.6 implies that it is directly proportional to  $\phi_{cB}$ :

$$\phi_{hB}^{\max} \propto \phi_{cB} \quad (4.7)$$

The proportionality constant is simply the ratio, which we denote  $R^{\max}$ . Since the minimization of the free energy reduces the number of independent variables to three,  $R^{\max}$  is predicted to be a function of  $\chi Z_{cB}$  and  $Z_{hB}/Z_{cB}$ . Physically, this means that the solubilization limit of the hB homopolymer is proportional to the cB content, and the proportionality constant depends on the relative degrees of polymerization,  $Z_{hB}/Z_{cB}$ , and on  $\chi Z_{cB}$ .

Figure 5 illustrates the calculated solubility limit, expressed as  $R^{\max}$ , for a model system for which the Kuhn statistical lengths are equal, i.e.,  $b_A = b_B$ , as are the two pure component densities,  $\rho_{0A} = \rho_{0B}$ , as a function of  $Z_{hB}/Z_{cB}$ , for different values of  $\chi Z_{cB}$ . There are two primary results indicated. First, there exist reasonable systems such that the total volume fraction of hB which can be solubilized is on the same order as the total initial cB content. Second,  $\phi_{hB}^{\max}/\phi_{cB}$  is a decreasing function of both

$\chi Z_{cB}$  and  $Z_{hB}/Z_{cB}$ . Consider the curve corresponding to  $\chi Z_{cB} = 20$ , which could correspond to  $\chi = 0.2$  and  $Z_{cB} = 100$ . For this case,  $\phi_{hB}^{\max} \approx \phi_{cB}$  for  $Z_{hB} \approx 20$ , and it falls by an order of magnitude as  $Z_{hB}$  increases by a factor of about 3. Increasing either  $\chi$  or  $Z_{cB}$  also reduces the solubility limit, for a given value of  $Z_{hB}/Z_{cB}$ .

For  $Z_{hB} \ll Z_{cB}$  in particular, it is also apparent that the variation of  $\phi_{hB}^{\max}/\phi_{cB}$  with  $Z_{hB}/Z_{cB}$  is approximately a power law dependence. Although this is less clear from the figure, for a given value of  $Z_{hB}/Z_{cB}$ , it also varies with  $\chi Z_{cB}$  approximately as a power law. This can be understood qualitatively by approximating the free energy expression, eq 4.6, under the assumption that the solubility is large,  $\phi_{hB}^{\max}/\phi_{cB} \gg 1$ , which is not unreasonable as long as  $Z_{hB}/Z_{cB} \ll 1$ . With this assumption, along with eq 3.22 for  $l_B^0$ , the free energy can be written to leading order in  $\phi_{hB}^{\max}/\phi_{cB}$  as

$$\Delta \bar{g} \approx \frac{\phi_{cB}}{Z_{cB}} \left\{ \Gamma (\chi Z_{cB})^{1/3} \left( \frac{\phi_{hB}^{\max}}{\phi_{cB}} \right)^{2/3} - \frac{2}{3} \ln \left( \frac{\phi_{hB}^{\max}}{\phi_{cB}} \right) - \frac{Z_{cB}}{Z_{hB}} \right\} \quad (4.8)$$

where  $\Gamma$  is simply a numerical factor. Setting  $\Delta \bar{g} = 0$  gives an approximate expression for  $\phi_{hB}^{\max}/\phi_{cB}$  which can be solved analytically if  $\ln(\phi_{hB}^{\max}/\phi_{cB}) \ll Z_{cB}/Z_{hB}$ . This results in

$$\frac{\phi_{hB}^{\max}}{\phi_{cB}} \propto (\chi Z_{cB})^{-1/2} \left( \frac{Z_{hB}}{Z_{cB}} \right)^{-3/2} \quad (4.9)$$

Although this simple result qualitatively summarizes the results of Figure 2, it should be emphasized that it is strictly valid only for the regime  $Z_{hB} \ll Z_{cB}$  and  $\phi_{hB}^{\max}/\phi_{cB} \gg 1$  and does not replace the numerical calculations of Figure 2. In fact, none of the systems of Figure 2 properly satisfies the second of these restrictions, resulting in the deviations from the strict power laws exhibited there.

Turning to the swollen micelle regime, since  $f = 1$  for all swollen micelles we can easily calculate their characteristics. The radius is simply

$$l_B \approx \left( 1 + \frac{\phi_{hB}}{\phi_{cB}} \right)^{1/3} l_B^0 \quad (4.10)$$

and the volume fractions within the cores are

$$\begin{aligned} \phi_{cB}^{(1)} &= \frac{\phi_{cB}}{\phi_{cB} + \phi_{hB}} \\ \phi_{hB}^{(1)} &= \frac{\phi_{hB}}{\phi_{cB} + \phi_{hB}} \end{aligned} \quad (4.11)$$

The number of micelles per unit volume and the number of copolymer molecules per micelle are the same as for the unswollen cases, given by eqs 3.24 and 3.25. The number of hB molecules per micelle is

$$N_{hB} = \left( \frac{8\pi^2 \chi}{27} \right)^{1/2} (\rho_0 b b_B^2) \frac{\phi_{hB}}{\phi_{cB}} \frac{Z_{cB}^2}{Z_{hB}} \quad (4.12)$$

These predictions have clear physical meanings. In a binary copolymer/homopolymer blend, the micelle core radii depend on  $\chi$  and  $Z_{cB}$ . Added homopolymer can be



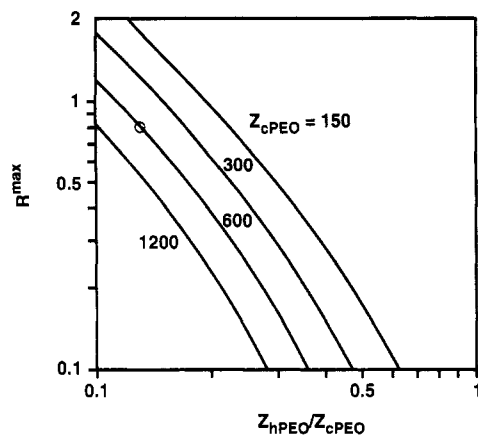


**Figure 6.** Calculated solubility limits of PEO homopolymer relative to the copolymer PEO content,  $R^{\max} = \phi_{\text{hPEO}}^{\max}/\phi_{\text{cPEO}}$ , as a function of the relative degrees of polymerization,  $Z_{\text{hPEO}}/Z_{\text{cPEO}}$ , for different values of  $Z_{\text{cPEO}}$ , as shown, with  $\chi = 0.3$ . The point indicated by the open circle at  $Z_{\text{hPEO}}/Z_{\text{cPEO}} = 0.13$  corresponds to the experimental system studied here.

solubilized within the micelle cores up to a limit which depends primarily on  $\chi Z_{\text{cB}}$  and the ratio  $Z_{\text{hB}}/Z_{\text{cB}}$ ; in particular, if  $Z_{\text{hB}}/Z_{\text{cB}} \ll 1$ , then the solubilization limit of the homopolymer is on the order of  $\phi_{\text{hB}}^{\max} \approx \phi_{\text{cB}}$ . Adding additional copolymer leaves the sizes of each micelle unchanged but creates more of them; by contrast, adding hB homopolymer does not affect the number of micelles but instead swells the existing ones. The core radius of each swollen micelle is determined by  $\chi$ ,  $Z_{\text{cB}}$ , and the ratio of homopolymer and copolymer volume fractions in the core,  $\phi_{\text{hB}}/\phi_{\text{cB}}$ .

**4.3. The PS/PS-*b*-PEO/PEO System: Theory and Experiment.** Turning to our specific system of interest, Figure 6 shows the solubility limits calculated for h-PEO in the ternary PS/PS-*b*-PEO/PEO mixture for different values of  $Z_{\text{cPEO}}$ . This is similar to Figure 5 but calculated using the appropriate reference densities and Kuhn lengths as for Figures 2 and 3 and with  $\chi = 0.3$ .

The results shown in Figure 6 are qualitatively similar to those in Figure 5, with quantitative differences due to the different reference densities. For example, the two uppermost curves of Figure 6 correspond to  $\chi Z_{\text{cB}} = 45$  and 90, which are similar to the two lower curves of Figure 5. Comparison of the two pairs of curves shows that, for a given value of  $Z_{\text{hB}}/Z_{\text{cB}}$ , the solubility limit for this system is greater than for the model system by about a factor of 2.

We have examined the morphology of a series of ternary mixtures of PS, PS-*b*-PEO, and PEO, using the PS-*b*-PEO(57.3/40.7)<sub>M</sub> copolymer. As indicated in section 2.1, the average degrees of polymerization are  $Z_{\text{cPEO}} \approx 600$ ,  $Z_{\text{cPS}} \approx 835$ ,  $Z_{\text{hPEO}} \approx 80$ , and  $Z_{\text{hPS}} \approx 1000$ . For this system, the model predicts a solubility limit of  $\phi_{\text{hB}}^{\max} \approx 0.8\phi_{\text{cB}}$ , which is indicated by the open circle on Figure 6. Given the simplifications of the theory and the small uncertainty in the value of  $\chi$ , this prediction should be taken as a guide that, for this system,  $\phi_{\text{hB}}^{\max} \approx \phi_{\text{cB}}$ .

Table 1 shows the compositions examined, the calculated size of PEO domains for the two compositions satisfying the condition  $\phi_{\text{hPEO}} \leq \phi_{\text{cPEO}}$ , and the size of PEO domains in each composition as observed in transmission electron micrographs. Figure 7 shows illustrative transmission electron micrographs for these compositions in which the micellar PEO cores and large PEO homopolymer domains are visualized by staining with phosphotungstic acid. Across the series, the total weight fraction of PEO (that

emanating from h-PEO and from PS-*b*-PEO) is held constant at 0.047.

The baseline composition in our study, sample 1-1, is comprised of 20% by weight of the PS-*b*-PEO dispersed in PS. Transmission electron micrograph (TEM) cross sections from  $\approx 50 \mu\text{m}$  films of this composite reveal homogeneously dispersed domains of PEO (micelle cores) ranging in diameter from 20 to 40 nm. These experimentally observed sizes correspond well with the 45 nm value predicted by the theory. Sample 2-1 is comprised of 10% by weight of PS-*b*-PEO and 2.4% by weight of homopoly(ethylene oxide) in PS. TEM cross sections from  $\approx 50 \mu\text{m}$  films of this composite reveal homogeneously dispersed PEO domains (micelle cores swollen with h-PEO) ranging in size from 20 to 60 nm. The observed size again corresponds well with the diameter of 60 nm predicted by the theory for a sample at its limiting composition of  $\phi_{\text{hPEO}} \approx \phi_{\text{cPEO}}$ .

Sample 3-1 is comprised of 5% by weight of PS-*b*-PEO and 3.5% by weight of h-PEO in PS. In this case, the relative volume fraction of h-PEO is 3 times the volume fraction of the c-PEO segment and exceeds the theoretically predicted micelle swelling limit of h-PEO by about a factor of 3. The TEM cross sections show homogeneously dispersed, polydisperse domains of PEO ranging in size from 40 to as large as 200 nm. The large domains must be comprised almost entirely of homopoly(ethylene oxide) and represent phase-separated h-PEO. The coexistence of the large domains with micelles of the same size as those in the binary PS-*b*-PEO/PS system is consistent with the prediction that, once a certain threshold concentration is reached, all of the PEO homopolymer is expelled into a second phase.

In samples 4-1 and 5-1, the h-PEO volume fractions exceed those of the c-PEO by factors of approximately 5 and 12, greatly exceeding the predicted solubilization limit. The polydispersity and maximum size of the observed domain diameters have become even more pronounced in these samples, with PEO domain structures as large as  $1 \mu\text{m}$ . The apparent absence of micelle-type domains in sample 5-1 reflects the very low copolymer content; the overall volume fraction of PEO due to the copolymer in this case is only about 0.001, a large proportion of which may well be localized at the homopolymer interfaces.

## 5. Summary

A simple theory of the swelling of micelles by solubilized homopolymer in dilute block copolymer/homopolymer blends and some supporting experimental evidence have been presented. The theory predicts the homopolymer solubilization limit as well as the micelle characteristics (size, number, and cmc). Specific calculations were carried out for binary PS/PS-*b*-PEO and ternary PS/PS-*b*-PEO/PEO blends, which are the systems studied experimentally by TEM. The observations support the predictions of the maximum volume of low molecular weight PEO which can be incorporated in PS-*b*-PEO micelles, as well as the micelle sizes and number densities.

For the theoretical picture, we developed a model of systems in at least metastable equilibrium, introducing a simple expression for the free energy. The expression is based on a similar picture developed earlier for copolymer micelles in a homopolymer matrix and incorporates the dominant factors controlling the sizes of the micelle cores and the solubility limit of homopolymers within the cores. It is developed explicitly for systems in which the overall copolymer volume fraction is considerably greater than the cmc but is low enough that micelles do not overlap and in which the homopolymers are incompatible.

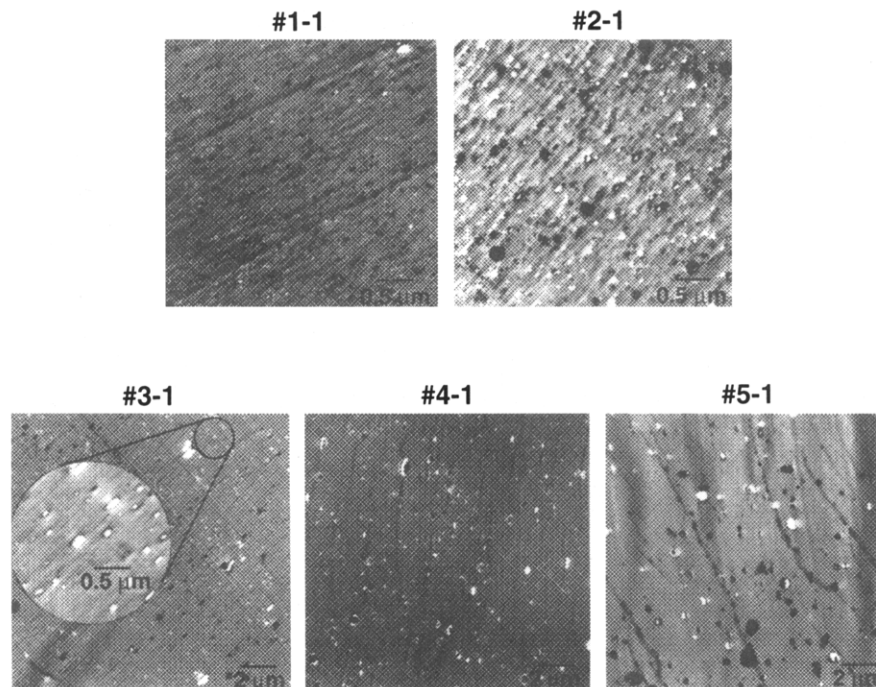


Figure 7. Illustrative micrographs for the PS/PS-*b*-PEO and PS/PS-*b*-PEO/PEO composites detailed in Table 1.

The conclusions of the model can be summarized as follows. For the binary A-*b*-B/A systems, the cmc depends strongly on the product  $\chi Z_{cB}$ , where  $\chi$  is the Flory interaction parameter and  $Z_{cB}$  is the degree of polymerization of the copolymer block which forms the cores. The radius of the core of each micelle and related quantities such as the number of molecules per micelle are also controlled primarily by  $\chi$  and  $Z_{cB}$ . Specifically, the radius scales approximately as  $l_B \propto \chi^{1/6} Z_{cB}^{2/3}$ , reflecting a balance between the interfacial tension at each core-corona interface and the stretching of the cB blocks. The addition of more copolymer leads to a concomitant increase in the number of density of micelles, with little change in the size of each of them.

In the ternary systems in which the copolymer forms micelles, the model predicts that hB homopolymer is solubilized in the cores up to a solubility limit which is directly proportional to the existing volume fraction of cB in the micelle cores,  $\phi_{hB}^{\max} \propto \phi_{cB}$ . For a given  $\phi_{cB}$ ,  $\phi_{hB}^{\max}$  is a decreasing function of  $\chi Z_{cB}$  and  $Z_{hB}/Z_{cB}$ . Typically, it decreases by at least an order of magnitude as  $Z_{hB}$  increases from  $Z_{hB} \simeq Z_{cB}/10$  to  $Z_{hB} \simeq Z_{cB}$ . The solubilization is due to the entropy associated with the low homopolymer concentrations localized within the micelle cores rather than the smaller volume associated with a separate hB phase. It is opposed by the increase in the stretching and interfacial energy of swollen micelles.

In contrast to the effects of added copolymer, added hB homopolymer swells existing micelles but does not change their number density. The radius of each micelle is controlled primarily by the degree of polymerization of the core-forming copolymer block,  $Z_{cB}$ , the relative volume fraction, through  $[1 + \phi_{hB}/\phi_{cB}]$ , and the temperature via the Flory  $\chi$  parameter.

These predictions imply that dispersions of B material can be tailored by using both copolymer and solubilized homopolymer. First, there exist reasonable systems for which a significant concentration of homopolymer can be solubilized. Second, the solubility limit and individual micelle sizes are controlled by both the copolymer and homopolymer, whereas the number of micelles per unit volume is controlled primarily by only the copolymer.

Specifically, the core radius scales approximately as  $l_B \propto \chi^{1/6} Z_{cB}^{2/3} [1 + \phi_{hB}/\phi_{cB}]^{1/3}$ , the solubility limit  $\phi_{hB}^{\max}$  is proportional to  $\phi_{cB}$  and decreases with increasing  $\chi Z_{cB}$  and increasing  $Z_{hB}/Z_{cB}$ , and the number of micelles per unit volume scales as  $n_M \propto \phi_{cB}/(\chi^{1/2} Z_{cB}^2)$ . Taken together, these imply that low molecular weight homopolymer will be solubilized best, as long as its molecular weight is not so low that it dissolves into the matrix.

**Acknowledgments.** We thank Dr. G. DiPaola-Baranyi for useful discussions and measurements of the value of  $\chi$  needed for this work. The efforts of the Xerox electron microscopy group (J. Czerniawski, H. Freitas, Jr., and T. Harper) in obtaining the TEM's are gratefully acknowledged. The research was supported in part by the Natural Sciences and Engineering Research Council of Canada.

## References and Notes

- (1) Noolandi, J.; Hong, K. M. *Macromolecules* **1982**, *15*, 482; **1983**, *16*, 1443.
- (2) Whitmore, M. D.; Noolandi, J. *Macromolecules* **1985**, *18*, 657.
- (3) Leibler, L.; Orland, H.; Wheeler, J. C. *J. Chem. Phys.* **1983**, *79*, 3550.
- (4) Leibler, L. *Macromolecules* **1980**, *13*, 1602.
- (5) Helfand, E.; Wasserman, Z. R. In *Developments in Block Copolymers*; Goodman, I., Ed.; Elsevier: New York, 1982; Vol. 1.
- (6) Hong, K. M.; Noolandi, J. *Macromolecules* **1981**, *14*, 727.
- (7) Fredrickson, G. F.; Helfand, E. *J. Chem. Phys.* **1987**, *87*, 697.
- (8) Vavasour, J. D.; Whitmore, M. D. *Macromolecules* **1982**, *25*, 5477.
- (9) Shull, K. *Macromolecules* **1992**, *25*, 2122.
- (10) Shull, K.; Winey, K. I. *Macromolecules* **1992**, *25*, 2673.
- (11) Mayes, A. M.; Olvera de la Cruz, M. *J. Chem. Phys.* **1991**, *6*, 4670.
- (12) Selb, J.; Marie, P.; Rameau, A.; Duplessix, R.; Gallot, Y. *Polym. Bull.* **1983**, *10*, 444.
- (13) Bluhm, T. L.; Whitmore, M. D. *Can. J. Chem.* **1985**, *63*, 249.
- (14) Xu, R.; Winnik, M. A.; Riess, G.; Chu, B.; Croucher, M. L. *Macromolecules* **1992**, *25*, 644.
- (15) O'Malley, J. J.; Marchessault, R. H. *Macromol. Synth.* **1972**, *4*, 35.
- (16) The effective Kuhn length entering this and other expressions is  $(bb_B^2)^{1/3}$ . To within the accuracy of the theory derived here, this could be replaced by  $b_B$ .

- (17) Brandrup, J.; Immergut, E. H., Eds. *Polymer Handbook*, 2nd ed.; Interscience: New York, 1975.
- (18) DiPaola-Baranyi, G.; Van Laeken, A. C.; Smith, T. W.; Luca, D. J. *33rd IUPAC International Symposium on Macromolecules*, 1990.
- (19) DiPaoli-Baranyi and Van Laeken et al. used 10 different probe molecules, each giving slightly different results. In principle, the value of  $\chi$  is expected to depend on the size of the probe molecule in a systematic manner; this dependence is similar to its dependence on  $\rho_0$  in the current model.<sup>20,21</sup> However, the variation did not follow the expected systematic behavior, and so we simply took their average value for the present work, independent of  $\rho_{0R}$ .
- (20) Deshpande, D. D.; Patterson, D.; Schreiber, H. P.; Su, C. S. *Macromolecules* **1974**, *7*, 530.
- (21) DiPaola-Baranyi, G.; Degré, P. *Macromolecules* **1981**, *14*, 1456.
- (22) Nagata, M.; Fukuda, T.; Inagaki, H. *Macromolecules* **1987**, *20*, 2173.
- (23) Hashimoto, T.; Tanaka, T.; Hasegawa, H. *Macromolecules* **1990**, *23*, 4378.
- (24) Tanaka, H.; Hasegawa, H.; Hashimoto, T. *Macromolecules* **1991**, *24*, 240.
- (25) Tanaka, H.; Hashimoto, T. *Macromolecules* **1991**, *24*, 5712.
- (26) Winey, K.; Thomas, E. L.; Fetters, L. J. *Macromolecules* **1991**, *24*, 6182.
- (27) Banaszak, M.; Whitmore, M. D. *Macromolecules* **1992**, *25*, 2757.
- (28) This assumption is easily relaxed and would need to be to calculate, for example, the corona thickness. However, for  $Z_{hA} \simeq Z_{cA}$  as in the experiments of interest here,  $\alpha_A \simeq 1$  and this correction would be very small.<sup>2</sup>